DOI: 10.61782/fa.2025.0096

FORUM ACUSTICUM EURONOISE 2025

# ACTIVE NOISE CONTROL WITH EXTENDED QUIET ZONES USING TIME-DOMAIN UNDERDETERMINED MULTICHANNEL INVERSE FILTERS AND KERNEL INTERPOLATION

**Michael Anthony**[1*] **Mingsian R. Bai**[1]
[1] Department of Electrical Engineering, National Tsing Hua University, Taiwan

**ABSTRACT**

This paper proposes a novel Active Noise Control (ANC) framework that exploits time-domain underdetermined multichannel inverse filters (TUMIF) with kernel-based sound field interpolation to enhance the spatial coverage of noise suppression. While TUMIF is effective in reducing noise at the measured control points, its performance degrades elsewhere, limiting its application in extended spatial regions. To solve this problem, a kernel ridge regression method is used to interpolate the Acoustic Transfer Functions (ATFs) of the secondary loudspeakers and the unmeasured control points, based on the Helmholtz equation. The interpolated control points enable the creation of extended quiet zones with a limited number of measured control points. The simulation results showed that the proposed approach achieved significant broadband noise reduction in an extended control region.

**Keywords:** *active noise control, sound field interpolation, kernel method.*

## 1. INTRODUCTION

Active Noise Control (ANC) is an effective technique for reducing unwanted noise, especially in the low frequency range, by generating anti-noise signals through secondary loudspeakers [1]. Adaptive filtering techniques, such as the widely used filtered-x least mean squares (FxLMS), handle time-varying issues but suffer from increasing computational complexity as the number of secondary loudspeakers and control points increases [1–2]. Moreover, these approaches are constrained by the overdetermined inverse filtering problem, which limits their achievable noise reduction performance. To address this, time-domain underdetermined multichannel inverse filtering (TUMIF) is introduced [3].

A major limitation of traditional ANC systems is that noise cancellation is confined to measured control points, with performance deteriorating in between these locations [4]. Broader quiet zones can be achieved by increasing the amount of measured control points. However, measuring a large number of measured control points is often impractical due to the time-consuming calibration process and physical constraints in real-world environment [5]. To overcome this challenge, the kernel ridge regression method [6] is proposed to estimate the Acoustic Transfer Functions (ATFs) at unmeasured locations, so-called interpolated control points. These interpolated control points enable broader noise suppression without requiring additional physical sensors.

In this work, we propose a novel ANC framework that integrates TUMIF with kernel interpolation to achieve spatially extended noise control. This combination enhances the noise suppression at interpolated control points while maintaining the performance at measured control points.

## 2. RELATED WORK

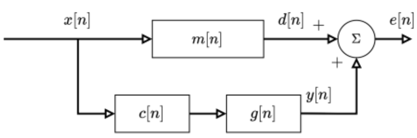


**Figure 1.** Block diagram of a single-channel feedforward ANC system.

*Corresponding author: michaelzhang220@gmail.com.

Single-channel feedforward ANC system can be seen as a model-matching problem as illustrated in Fig. 1. Under the assumption that both the secondary path $g[n]$ and the controller $c[n]$ are FIR systems, their linear convolution should match the primary path $m[n]$ such that the residual error signal $e[n]$ tends to zero, with $n$ denoting the discrete time index. Let $L_p$, $L_s$, and $L_c$ be the impulse response length of, respectively, primary path, secondary path, and controller, the matrix form of the linear convolution relation is modeled as

$$\mathbf{Gc} = -\mathbf{m} \quad (1)$$

where

$$\mathbf{m} = [m[0] \quad m[1] \quad \cdots \quad m[L_p - 1]]^T \quad (2)$$

$$\mathbf{c} = [c[0] \quad c[1] \quad \cdots \quad c[L_c - 1]]^T \quad (3)$$

$$\mathbf{G} = \begin{bmatrix} g[0] & 0 & \cdots & 0 \\ g[1] & g[0] & & \vdots \\ \vdots & g[1] & \ddots & \\ g[L_s - 1] & \vdots & & 0 \\ 0 & g[L_s - 1] & & g[0] \\ \vdots & 0 & \ddots & g[1] \\ & \vdots & & \vdots \\ 0 & 0 & \cdots & g[L_s - 1] \end{bmatrix} \quad (4)$$

Note that $L_p = L_s + L_c - 1$ and $\mathbf{G}$ is a $L_p \times L_c$ convolution matrix. The least square (LS) solution is computed as:

$$\mathbf{c}_{LS} = -\mathbf{G}^{+}\mathbf{m} = -\left(\mathbf{G}^T\mathbf{G}\right)^{-1}\mathbf{G}^T\mathbf{m} \quad (5)$$

The fact that Eqn. (1) is an overdetermined system ($L_p > L_c$) generally leads to a non-zero minimum residual error. The TUMIF approach [3] has proven effective in mitigating this problem by introducing additional secondary loudspeakers.

## 3. PROPOSED METHOD

The proposed method is divided into two stages: calibration stage and testing stage. At the calibration stage, the ATFs between $J$ microphones and $K$ secondary loudspeakers $G_F$ are measured. ATFs at interpolated control points $\hat{G}_F$ are estimated using kernel ridge regression based on the measured one and then inverse transformed into time-domain impulse reponses (IRs). Both the interpolated and measured IRs are fed onto TUMIF to compute the coefficients of the controllers $\mathbf{c}$. The microphones are detached at the testing stage and the proposed ANC framework suppresses unwanted noise in a widened region, resulting in broader quiet zones.

### 3.1 Sensor interpolation using kernel method

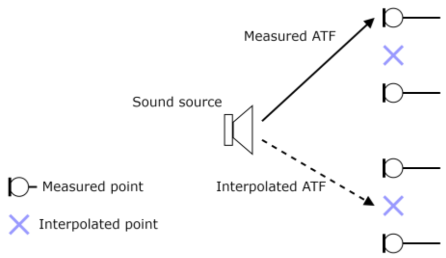


**Figure 2**. Block diagram of the sensor interpolation problem.

As shown in Fig. 2, kernel interpolation is utilized to estimate the ATFs in between measured control points, as written as the following optimization problem:

$$\min_{\hat{G}_F} \Im = \sum_{j=1}^{J} \left|\hat{G}_F(\mathbf{r}_j) - G_F(\mathbf{r}_j)\right|^2 + \alpha \left\|\hat{G}_F\right\|_{\mathcal{H}}^2 \quad (6)$$

where $\hat{G}_F(\mathbf{r}_j)$ and $G_F(\mathbf{r}_j)$ are, respectively, the interpolated and measured ATFs at position vector $\mathbf{r}_j$ of the $j$ microphone, $\alpha$ is the regularization parameter, and $\|\bullet\|_{\mathcal{H}}^2$ is the squared $L_2$-norm within the Hilbert space $\mathcal{H}$. By deriving the reproducing kernel, the solution of Eqn. (6) can be obtained as [6]

$$\hat{G}_F(\mathbf{r}) = \kappa^T(\mathbf{r})\left(\mathbf{K} + \alpha\mathbf{I}_J\right)^{-1}\mathbf{G}_F \quad (7)$$

where

$$\mathbf{K} = \begin{bmatrix} j_0\left(k\|\mathbf{r}_1 - \mathbf{r}_1\|_2\right) & \cdots & j_0\left(k\|\mathbf{r}_1 - \mathbf{r}_J\|_2\right) \\ \vdots & \ddots & \vdots \\ j_0\left(k\|\mathbf{r}_J - \mathbf{r}_1\|_2\right) & \cdots & j_0\left(k\|\mathbf{r}_J - \mathbf{r}_J\|_2\right) \end{bmatrix} \quad (8)$$

$$\kappa^T(\mathbf{r}) = \left[j_0\left(k\|\mathbf{r} - \mathbf{r}_1\|_2\right) \quad \cdots \quad j_0\left(k\|\mathbf{r} - \mathbf{r}_J\|_2\right)\right] \quad (9)$$

are the Gram matrix and kernel function, respectively, in which $k$ is the wave number, $\mathbf{I}_J$ denotes the $J \times J$

identity matrix, $\mathbf{r}$ is position vector of the interpolated control point, and $j_0(\bullet) = \sin(\bullet)/(\bullet)$ denotes the zeroth-order spherical Bessel function, also known as the sinc function.

### 3.2 TUMIF

Let $J_t$ be the total number of both interpolated and measured control points. The multichannel version of Eqn. (1) can be formulated as

$$\begin{bmatrix} \mathbf{G}_{11} & \cdots & \mathbf{G}_{1K} \\ \vdots & \ddots & \vdots \\ \mathbf{G}_{J_t 1} & \cdots & \mathbf{G}_{J_t K} \end{bmatrix} \begin{bmatrix} \mathbf{c}_1 \\ \vdots \\ \mathbf{c}_K \end{bmatrix} = \begin{bmatrix} -\mathbf{m}_1 \\ \vdots \\ -\mathbf{m}_{J_t} \end{bmatrix} \tag{10}$$

where

$$\mathbf{m}_j = [m_j[0] \quad m_j[1] \quad \cdots \quad m_j[L_p - 1]]^T \tag{11}$$

$$\mathbf{c}_k = [c_k[0] \quad c_k[1] \quad \cdots \quad c_k[L_c - 1]]^T \tag{12}$$

$$\mathbf{G}_{jk} = \begin{bmatrix} g_{jk}[0] & \cdots & 0 \\ g_{jk}[1] & & \vdots \\ \vdots & \ddots & 0 \\ g_{jk}[L_s - 1] & & g_{jk}[0] \\ 0 & \ddots & g_{jk}[1] \\ \vdots & & \vdots \\ 0 & \cdots & g_{jk}[L_s - 1] \end{bmatrix} \tag{13}$$

for $j = 1, 2, \ldots, J_t$ and $k = 1, 2, \ldots, K$.

An underdetermined system can be established if the following requirement is satisfied:

$$L_p = L_s + L_c - 1 < KL_c \tag{14}$$

or

$$L_c > \frac{L_s - 1}{K - 1} \tag{15}$$

By satisfying Eqn. (15), exact solutions that result in zero residual errors exist. It also follows that an infinite number of exact solutions exists, providing additional freedom to achieve other objectives [3]. The minimum-norm solution can be wriitten as

$$\mathbf{c}_{LS} = -\mathbf{G}^{+}\mathbf{m} = -\mathbf{G}^T \left(\mathbf{G}\mathbf{G}^T\right)^{-1} \mathbf{m} \tag{16}$$

However, the Gram matrix $\mathbf{G}^T\mathbf{G}$ may be ill-posed at some frequencies, resulting in high gain controllers. This problem can be mitigated, at some cost in model fitting performance, by using the TIKR approach [7]

$$\mathbf{c}_{TIKR} = -\left(\mathbf{G}^T\mathbf{G} + \beta^2\mathbf{I}\right)^{-1} \mathbf{G}^T\mathbf{m} \tag{17}$$

where $\beta$ is the regularization parameter.

## 4. SIMULATION

### 4.1 Simulation setup

A $4 \times 4 \times 3$ m$^3$ rectangular room is considered in this simulation. Fig. 3(a) illustrates the location of primary loudspeaker (grey circle), secondary loudspeakers (blue circles), measured control points (red circles), and interpolated control points (red crosses). As displayed in Fig. 3(b), the loudspeakers are located one meter above the ground and another 30 cm higher for the microphones to mimic laptop user behavior. The ATFs are generated by using Image Source Method (ISM) [8] with a reverberation time (T60) of 120 ms and white noise is used as the primary noise.

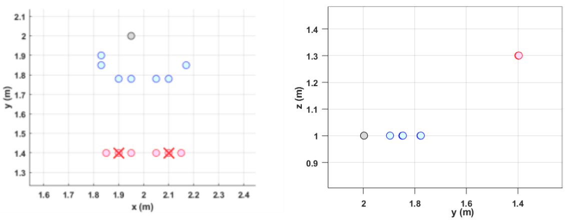


(a) (b)

**Figure 3**. Loudspeakers and microphones placement (a) *x* and *y* axes and (b) *y* and *z* axes.

The control points are numbered incrementally to the right starting from the first red circle on the left. The kernel interpolation parameter $\alpha$ and regularization parameter $\beta$ are set as, respectively, $10^2$ and $10^{-4}$. The $L_p$, $L_s$, and $L_c$ are configured as, respectively, 1024, 512, and 1024.

In order to verify the performance, MSNR [9] is used as the evaluation metric which is defined as

$$MSNR = 10\log_{10} \frac{\sum_{n=0}^{N} \left|d_j[n]\right|^2}{\sum_{n=0}^{N} \left|e_j[n]\right|^2} \tag{18}$$

where $d_j[n]$ and $e_j[n]$ represent the primary noise signal and and the error signal at the *j*-th control point. The larger the MSNR, the better the noise control performance.

### 4.2 Simulation results

Tab. 1 presents the MSNR values measured on each control point, comparing the performance of the proposed method with TUMIF. The combination of TUMIF and kernel interpolation achieves better performance at the unmeasured control points while maintaining its effectiveness at the measured control points. The power spectrum density (PSD) is plotted in Fig. 4, demonstrating that the proposed method controls noise more effectively than TUMIF.

**Table 1.** Comparison of MSNR (dB).

| Control points | TUMIF | Proposed method |
|---|---|---|
| Measured #1 | 28.88 | 31.12 |
| Unmeasured #2 | -27.72 | 8.49 |
| Measured #3 | 27.63 | 26.68 |
| Measured #4 | 28.15 | 27.32 |
| Unmeasured #5 | -22.5 | 4.22 |
| Measured #6 | 29.43 | 30.52 |

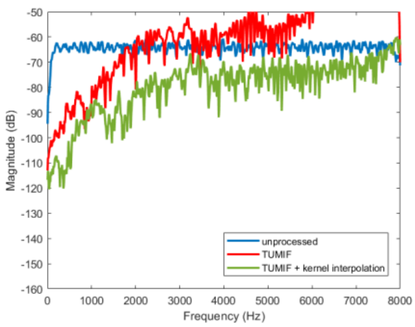


**Figure 4.** Power Spectrum Density (PSD) at unmeasured control point #2.

## 5. CONCLUSIONS

This study explored the integration of TUMIF with kernel interpolation to extend the quiet zone beyond measured control points. While TUMIF effectively suppresses noise at these points, its performance degrades at unmeasured locations. Kernel ridge regression was employed to interpolate ATFs, enabling broader noise suppression without additional physical microphones. Simulations demonstrated significant noise reduction at both measured and unmeasured control points for the proposed method, leading to an extended quiet zone. Real-time validation will be conducted in future work.

## 6. REFERENCES


[1] Y. Kajikawa, W.-S. Gan and S. M. Kuo, "Recent applications and challenges on active noise control," in *8th International Symp. on Image and Signal Processing and Analysis*, Trieste, Italy, 2013.

[2] P.-L. Zhong, Y.-S. Chen and M. R. Bai, "Multichannel learning-based spatially extended active noise control via model matching and sensor transfer function interpolation," in *Asia Pacific Signal and Information Processing Association Annual Summit and Conference*, Taipei, Taiwan, 2023.

[3] M. R. Bai, H.-Y. Chen, L. Yang and S.-C. Huang, "Active control of noise in a duct using the sparsely coded time-domain underdetermined multichannel inverse filters," *The Journal of the Acoustical Society of America,* vol. 146, no. 2, pp. 1371-1381, 2019.

[4] H. Ito, S. Koyama, N. Ueno and H. Saruwatari, "Feedforward spatial active noise control based on kernel interpolation of sound field," in *International Conference on Acoustics, Speech, and Signal Processing*, Brighton, UK, 2019.

[5] W.-L. Lin, Y.-S. Chen, B.-R. Lai and M. R. Bai, "Multichannel room response equalization with a broadened control region using a linearly constrained approach and sensor interpolation," *The Journal of the Acoustical Society of America,* vol. 153, no. 4, pp. 1960-1973, 2023.

[6] N. Ueno, S. Koyama and H. Saruwatari, "Kernel ridge regression with constraint of helmholtz equation for sound field interpolation," in *International Workshop on Acoustic Signal Enhancement*, Tokyo, Japan, 2018.

[7] A. N. Tikhonov, "Solution of nonlinear integral equations of the first kind," *Dokl. Akad. Nauk SSSR,* vol. 156, no. 6, pp. 1296-1299, 1964.

[8] J. B. Alley and D. A. Berkley, "Image method for efficiently simulating small-room acoustics," *The Journal of the Acoustical Society of America,* vol. 65, no. 4, pp. 943-950, 1979.

[9] D. P. Das and G. Panda, "Active mitigation of nonlinear noise processes using a novel filtered-s LMS algorithm," *IEEE Transactions on Speech and Audio Processing,* vol. 12, no. 3, pp. 313-322, 2004.